CRYSTAL GROWTH & DESIGN

ARTICLE

pubs.acs.org/crystal

Alkali-Assisted, Atmospheric Plasma Production of Titania Nanowire Powders and Arrays

Vivekanand Kumar,[†] Jeong H. Kim,[†,‡] Jacek B. Jasinski,[†] Ezra L. Clark,[†,‡] and Mahendra K. Sunkara*[,†]

[†]Conn Center for Renewable Energy Research and Chemical Engineering Department, University of Louisville, Louisville, KY 40292, United States

[‡]Advanced Energy Materials, LLC, 201 East Jefferson Street, Louisville, Kentucky 40202, United States

Supporting Information

ABSTRACT: We report a new ultrafast (reaction time on the scale of a minute) gas-phase method for synthesizing highly crystalline titanate phase nanowires (NWs) using oxidation of either Ti metal (foils or powders) or spherical TiO_2 powders with an atmospheric pressure microwave plasma. In this method, alkali metal compounds of Li, Na, and K are shown to form molten alloys of alkali metal-Ti-O during plasma exposure. Bulk nucleation and subsequent basal growth of the resulting nuclei from the molten alkali metal-Ti-O resulted in the respective titanate NWs. The current state-of-the-art methods involve long reaction time scales (~1 day) for synthesis of TiO_2 NWs.

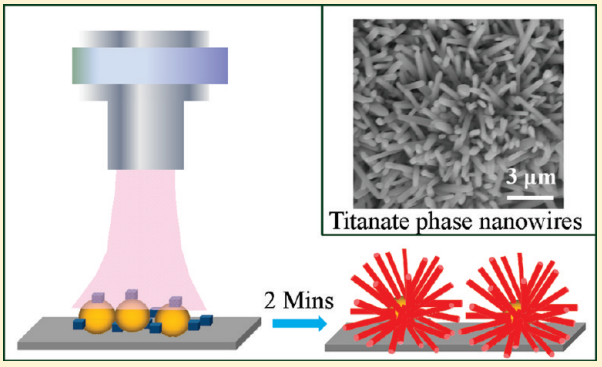

INTRODUCTION

TiO_2 is one of the most widely studied oxide materials because of its important applications in dye-sensitized solar cells,[1] Li-ion batteries,[2] gas sensing,[3] and water-splitting[4] owing to its superior properties such as low toxicity, environmental safety, chemical stability, favorable mechanical properties, large band gap (3.2 eV anatase), and high refractive index (n = 2.4). Currently sintered TiO_2 nanoparticles (NPs) are prominently used in many of the above energy conversion devices because of their availability and manufacturability in large amounts (from traditionally known particle production techniques). However, NWs are predicted to have better inherent charge transport properties because of single crystalline pathways for both surface and bulk charge transport compared to sintered NPs. As an example, the charge transport through SnO_2 NWs is an order of magnitude better than that within its NPs counterparts.[5] One would require large amounts (hundreds of grams or kilograms) of TiO_2 NWs for realization of any of the energy conversion applications. But the current methods of producing TiO_2 NWs are limited to producing only a few milligrams in a batch.

Early efforts on the synthesis of one-dimensional (1D) nanostructures of TiO_2 (nanotubes (NTs)) used electro deposition and sol−gel methods inside anodic alumina membrane (AAM) templates.[6,7] Subsequently, template-free hydrothermal synthesis of TiO_2 NTs and NWs using sodium hydroxide reflux was reported.[8,9] In fact, much of the progress in TiO_2 NW synthesis happened with hydrothermal methods[2,10−12] which employ high pressure conditions (in an autoclave) over a long time resulting in a small amount of product (1 g/day). Also the growth mechanism responsible for the observed 1D growth is not clear. Most importantly, it is not clear about scalability toward bulk production due to long reaction times involved (~1 day).

Gas phase synthesis of TiO_2 NWs is ideal for scale-up toward mass production. However, the direct gas phase oxidation (of metal foils or powders using plasma) approach to obtain metal oxide NWs has only been limited to low-melting point metals (e.g., Ga, Sn, Zn, etc.)[13,14] and certain high melting point metals such as (Nb,[15] V,[15] and Fe,[16]). It does not work in the case of Ti foil due to its high melting point (1668 °C), rapid oxidation to form oxide film, and/or production of oxide vapors. Recently, there have been a few attempts at synthesizing substrate based TiO_2 NWs. Experiments using horizontal tubular thermal evaporation methods, which operate by placing Ti metal powder upstream at 1050 °C and placing TiO_2 seeded alumina substrate downstream at 850 °C, resulted in TiO_2 NWs.[17] The use of Au or Cu layer coating onto substrates also resulted in TiO_2 NWs.[18,19] Also, a gas phase substrate-free synthesis attempt of TiO_2 NWs using microwave plasma torch via decomposition of titanium tetrachloride ($TiCl_4$) did not result in good quality NWs, similar to the results from other studies described above.[20] Thus, it is a challenge to produce large amounts (grams or kilograms) of unagglomerated TiO_2 NWs reliably using techniques known so far.

In our earlier studies, the use of halides in the form of alkali metal halides improved the selectivity of silicon NW formation

Received: January 16, 2011
Revised: April 24, 2011
Published: May 10, 2011

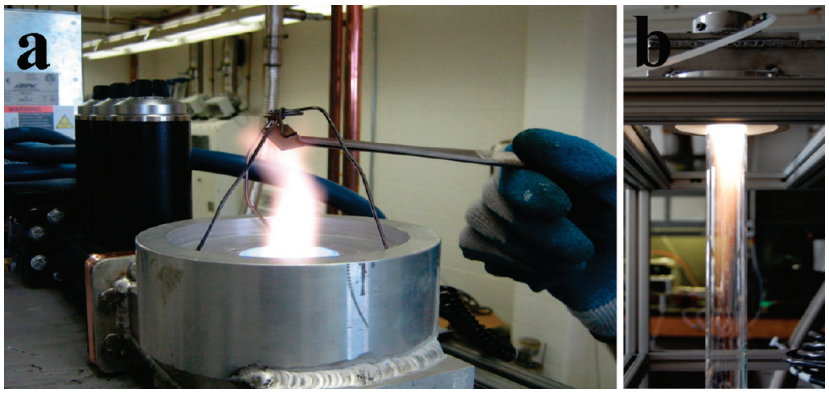

Figure 1. Photograph of atmospheric microwave plasma discharge generated using 1 kW power: (a) upward, open flame-like condition for foil exposure experiments; and (b) downward, inside quartz tube condition for powder experiments.

using low-melting metals such as Ga.[14] Similarly, the oxidation of Ti foils using KCl in the presence of moisture (similar to the hydrothermal technique) in a low pressure furnace at high temperatures over 24 h period resulted in K-doped TiO_2 NWs.[21] These experiments are similar to the hydrothermal synthesis except for the lower pressures used. Irrespective of the pressures used, both methods are limited due to their long reaction times involved.

In this paper, we describe a simple, ultrafast, and new method to synthesize TiO_2 NWs in the gas phase in the presence of a variety of alkali metals using either Ti foils and/or powders or TiO_2 powders. This method is fast (~1−5 min of reactions times scales) and easier to scale up for bulk production of TiO_2 NWs. The study demonstrates for the first time the direct conversion of TiO_2 NPs to TiO_2 NWs using gas phase oxidation which should be cost-effective for bulk manufacturing. Most importantly, various experimental observations are used to understand the underlying principle of nucleation and 1D growth of TiO_2 NWs in the presence of alkali metals.

EXPERIMENTAL SECTION

Experiments were performed using a newly designed microwave plasma reactor whose details have been described in detail elsewhere.[22,23] Briefly, the reactor is capable of producing highly dense microwave plasma discharges at powers ranging from 500 W to 3 kW at atmospheric conditions. The plasma flame can be shaped vertically upward (for foil exposure experiments as shown in Figure 1a) or downward (for powder feeding experiments as shown in Figure 1b) depending upon the requirement. A gaseous mixture of 2 lpm Ar, 11 lpm air, and 1000 sccm H_2 was fed at the top of the reactor to ignite and maintain the plasma throughout the experimental duration. A 1 × 1 cm piece of Ti foil was cut from a Ti foil (100 × 100 mm, 0.5 mm thick, from Alfa Aesar) and filed on both sides using a rectangular file and ultrasonicated for 5 min to clean the surface. A small amount of Ti powder (65 μm size) was mixed with alkali metal salt crystal and sprinkled together on the top of the Ti foil, which was then carefully exposed to the plasma flame at power of 800−1000 W (Figure 1a) for about 5 min. In direct gas phase synthesis experiments, metal or metal oxide powder mixed with alkali salt crystals was poured from the top of the reactor and collected at the bottom in a cup. The as-synthesized material was then dipped in 1 M HCl solution for 1 h for ion exchange, washed with deionized water, and annealed by exposure to plasma flame for 5 min. The material was characterized using a field emission scanning electron microscope (FE-SEM) (FEI Nova 600), an X-ray diffraction (XRD) (Bruker D8 Discover), a Renishaw in-via micro-Raman/photoluminescence spectroscope, and a transmission electron microscope (TEM) (Tecnai F20 FEI TEM).

RESULTS AND DISCUSSION

Experiments on direct gas phase oxidation by pouring Ti powder with no foreign metals from the top of the reactor in a setup as shown in Figure 1b resulted in TiO_2 NPs instead of NWs. Similar experiments using other metals such as Sn, Zn, and Al powders resulted in NWs.[22] In this regard, the results with TiO_2 are different and can be explained using gas−solid equilibrium thermodynamics and the corresponding metal oxide vapor pressures. Ti metal is prone to oxidation because of exothermic heat of reaction ($Ti(s) + 2O \rightarrow TiO_2(s)$, $\Delta H = -1445$ kJ/mol), and it forms a large amount of TiO_2 vapor plume as soon as it is poured in the quartz tube resulting in deposition on the tube walls. Theoretical gas phase equilibrium mole fraction calculations (EQUIL code using CHEMKIN Software by Reaction Design Inc., San Diego, CA) also confirmed that the TiO_2 is the preferred species both in the solid and vapor phase in O_2 excess conditions (Ti/O_2 molar ratio < 1) at temperatures ranging from 1000 to 2500 K. TiO_2 mole fraction is at least 10^9 and 10^{21} times higher than TiO and Ti respectively favoring TiO_2 NPs formation. The data are included in the Supporting Information, Figure S1.

In order to perform experiments to oxidize molten Ti particles without formation of oxide vapor plume, a set of experiments were conducted using lower plasma powers of 500 W, 100 sccm H_2, and 7 lpm air. These experiments resulted in 1D "nanowire-like" structures (~1 μm length) of TiO_2 in a flowery pattern. However, the results with such experiments were nonreproducible. Experiments were also conducted by exposing Ti foils to atmospheric plasma flame in a setup as shown in Figure 1a. Only short nanorods were obtained in some cases. The data are included as Figure S2a,b in the Supporting Information.

Experiments that mimic the hydrothermal synthesis technique were conducted using plasma oxidation in the presence of alkali metal compounds. In these experiments, Ti source (such as Ti metal powder of 65 μm size, and TiO_2 powder) mixed with alkali metals compounds (e.g., KCl) in a 50:50 wt % ratio was supported on Ti foil and was exposed to microwave plasma power of 800−950 W and 11 lpm of air for short periods of 2−5 min in a setup as shown in Figure 1a. These experiments resulted in a high density of NWs (>50 μm in length) in an array form emanating vertically from foils (top and cross-sectional view shown in Figure 2a,b) and radially from spherical particles as shown in

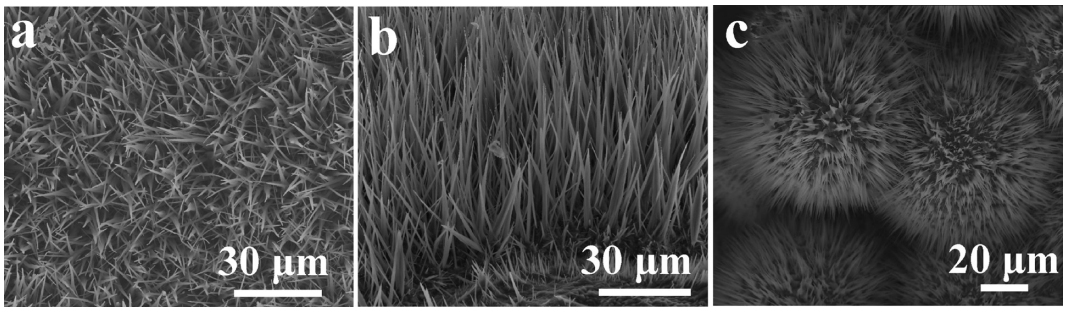

Figure 2. SEM image showing as-synthesized NWs obtained with plasma oxidation of Ti foil in the presence of sprinkled KCl: (a) top view and (b) cross-sectional view. (c) SEM image showing NWs obtained with plasma oxidation of Ti metal powder mixed with KCl supported on Ti foil.

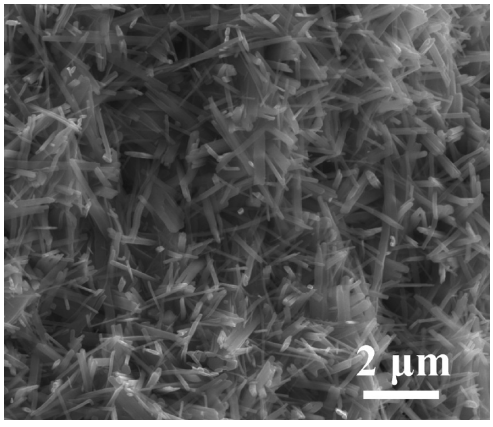

Figure 3. SEM images of as-synthesized NWs obtained after plasma exposure of TiO_2 powder and KCl mixture placed on a Ti foil.

Figure 2c. Samples shown in Figure 2a,c were synthesized in the same condition except that the sample used for Figure 2a is obtained directly on Ti foil, whereas the one in Figure 2c is obtained by placing Ti powder on Ti foil. The results with plasma exposure of TiO_2 powder (32 nm size, anatase) and KCl mixture on Ti foil showed complete conversion of spherical particles into straight NWs (Figure 3) similar to above experiments shown in Figure 2a. TiO_2 NPs are cheaper and readily available commercially and hence better as raw material for commercial scale production of TiO_2 NWs. Similar experiments done using Ti metal powders mixed with KCl supported on Fe foil (instead of Ti foil) resulted in similar result with flowery pattern of NWs from individual Ti metal powders. The Fe foil merely provides the support needed for proper mixing of Ti and alkali sources. This clearly shows that Ti substrate is not essential for NW formation, but it only facilitates proper mixing of the reagents. Results from these experiments suggest that NW synthesis requires (1) Ti source, (2) alkali metal reagent, and (3) proper contact and mixing between these upon plasma exposure.

The scalability of the above technique can only be established when NWs are obtained through direct gas phase oxidation experiments in a vertical plasma reactor (without the support of any substrate) using spherical TiO_2 or Ti metal powders. So, experiments were performed by pouring Ti or TiO_2 powders mixed with KCl crystals (50:50 wt %) at the top of the reactor using similar experimental conditions as those used for the data (foil exposure experiments) shown in Figure 2b. NWs resulted using sub-micrometer scale TiO_2 powder as feedstock and were not obtained when using sub-100 μm size Ti metal powders because of enhanced mixing and better contact with smaller size TiO_2 powders. These experiments using sub-micrometer size TiO_2 powders were converted to NW powders with 5% efficiency. At the same time, the experiments using TiO_2/KCl mixture in a boron nitride (BN) crucible exposed to plasma under similar conditions resulted in more efficient conversion to NWs (over 20% fraction in resulting powders). In the above experiments using crucible supported powders, the resulting NWs were shorter in length (about micrometer) and 100 nm diameter (Figure S3 shown in Supporting Information). The short lengths were due to smaller residence time (<1 s) and less feed mixture contact in direct gas phase set up. The plasma flame in this reactor can treat about 3−5 g/min of feed powder and can produce about 1 kg/day of NWs which can be achieved either in a direct gas phase or by using a conveyor belt type setup.

Experiments were also conducted to understand the factors affecting the morphology (diameter and density) of the resulting NWs by varying plasma parameters, exposure time, amount of KCl, and gas flow ratio (H_2/Air). The NW diameter and length increased when the KCl to Ti powder ratio was high and vice versa. In the experiments using spherical Ti powders, the addition of higher KCl amount resulted in higher density of NWs (compared to the result in Figure 2c) growing radially and laterally as shown in Figure 4a. Experiments conducted by adding H_2 to other feed gases resulted in thinner diameter NWs. Plasma exposure time variation experiments were not reproducible because of very fast reaction time scales (2−5 min), but 5 min was the best exposure time for good quality NWs. Experiments using higher plasma power seem to degrade the Ti sphere surface making the resulting NWs random in all directions (Figure 4b).

The as-synthesized NWs contained about 6−7 at % of K determined using an energy-dispersive X-ray spectroscopy (EDX) technique. There was no tip or amorphous oxide sheath around the wire and K incorporation was observed throughout the NW (Figure S4 in Supporting Information). Also, Cl was not seen because it is expunged in the gaseous form during the plasma exposure. High resolution TEM (HRTEM) and selected area electron diffraction (SAED) analysis in Figure 5a along with EDX revealed that the as-synthesized NWs are of $K_2Ti_8O_{17}$ monoclinic phase with a single crystalline layered structure. From SAED, the planes normal to NW growth direction are (200) planes with interplanar spacing of 7.8 Å that matches with the reported values of d_{200} for $K_2Ti_8O_{17}$.[21,24,25] The growth direction of the resulting

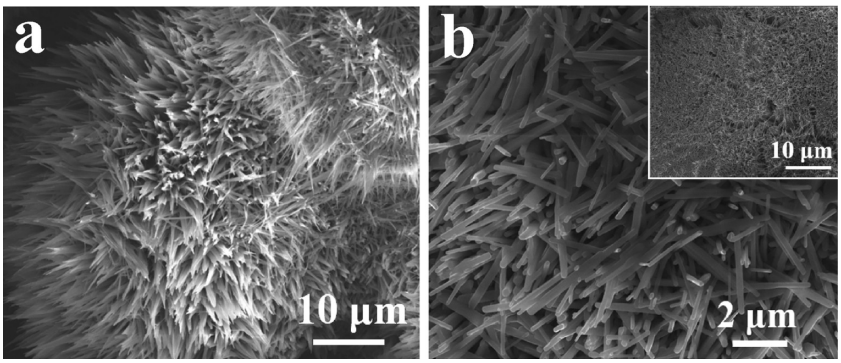

Figure 4. SEM images showing the effect of the (a) addition of a large amount of KCl with Ti powder onto Ti foil; and (b) plasma power with a longer exposure time (10 min) resulting in degraded Ti sphere (inset) with randomly oriented NWs.

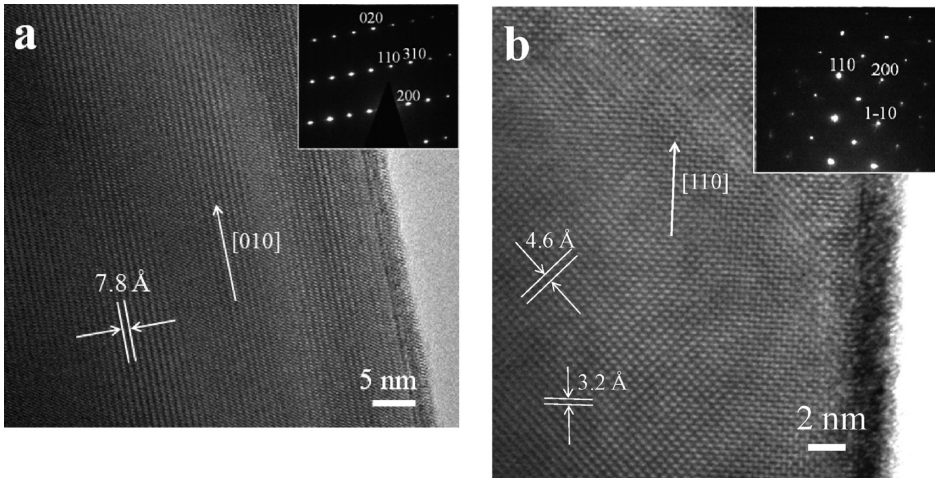

Figure 5. HRTEM image of (a) as-synthesized titanate NWs and (b) rutile TiO_2 NWs obtained after ion exchange and annealing along with their respective SAEDs in the inset.

titanate NWs is [010]. A typical hydrothermal reaction using Ti source such as TiO_2 powder or Ti foil and KOH can be represented by reactions 1[26] and 2 (as deduced from ref 12 for reaction involving sodium titanates), respectively.

$$8TiO_2\ (s) + 2KOH\ (l) \rightarrow K_2Ti_8O_{17}\ (s) + H_2O \quad (1)$$

$$8Ti\ (s) + 2KOH\ (l) + 15H_2O \rightarrow K_2Ti_8O_{17}\ (s) + 16H_2 \quad (2)$$

whereas the plasma exposure of TiO_2 powder in the presence of alkali compounds, for example, KOH or KCl can be expressed by reactions 3 and 4, respectively.

$$8TiO_2\ (s) + 2KOH\ (l) + O \rightarrow K_2Ti_8O_{17}\ (s) + H_2O + 0.5O_2 \quad (3)$$

$$8TiO_2\ (s) + 2KCl\ (l) + O \rightarrow K_2Ti_8O_{17}\ (s) + Cl_2 \quad (4)$$

Here reaction 3 is more spontaneous and favorable than reaction 1 by 174.6 kJ/mol based on ΔG calculations at 1200 K. Comparing reactions 3 and 1, it is clear that the presence of more reactive O species (compared to hydroxyl ion in reactions 1 and 2) provided by plasma exposure in reaction 3 plays a significant role here in making the reaction 3 more favorable. Also in both reactions 3 and 4, O in LHS can also be contributed from a combination of ($O^+ + e$ or $O^{2+} + 2e$) and KCl from a combination of ($K^+ + Cl^-$ or $K^+ + Cl + e$ or $K + Cl^+ + e$). It is the creation of such radicals in a highly dense microwave plasma discharge and their participation in the reactions 3 and 4 which makes it highly spontaneous. For example, replacing O with $O^+ + e$ and $O^{2+} + 2e$ make reactions 3 and 4 more spontaneous and favorable (i.e., more negative) by 1286 and 789 kJ/mol based on ΔG calculations at 1200 K. Similarly replacing KCl with $K^+ + Cl^-$ or $K^+ + Cl + e$ or $K + Cl^+ + e$ make reactions 3 and 4 more spontaneous by 460, 759, and 1593 kJ/mol respectively based on ΔG calculations at 1200 K.

There is a well-established procedure for converting sodium titanate nanowires to TiO_2 phase NWs by ion exchange in acids followed by annealing at high temperatures.[11,12] But such procedure was not reported for potassium titanate NWs. Also, the annealing step at high temperatures is typically conducted for times ranging from 3 to 6 h. In our case, the resulting titanate NWs were reacted with dilute HCl (1 M) for 1 h similar to the reported procedure.[11,12] The ion-exchange reaction can be represented by reaction 5

$$K_2Ti_8O_{17}NW + 2HCl\ (l) \rightarrow H_2Ti_8O_{17}NW + 2KCl\ (s) \quad (5)$$

In the following step (reaction 7), here the resulting product was annealed using exposure to the same atmospheric plasma setup for approximately 5 min or less instead of thermal annealing

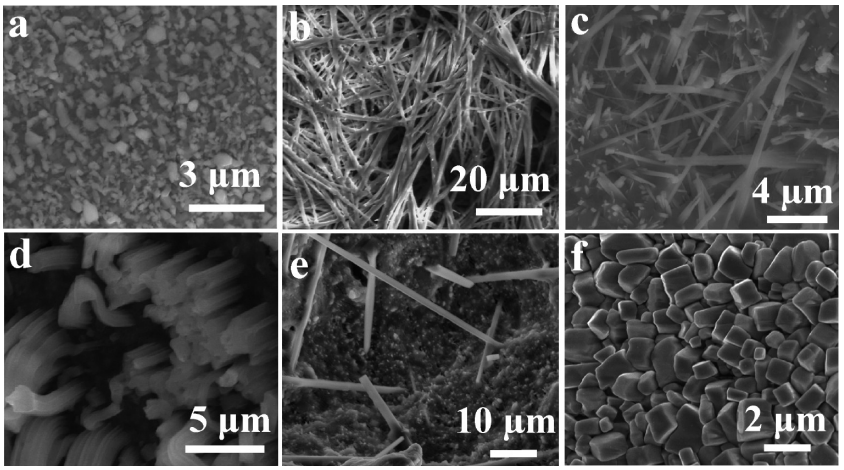

Figure 6. SEM images showing the effect of (a) HCl, (b) KOH, (c) NaCl, (d) LiCl, (e) NaOH, and (f) $CaCl_2$ placed on Ti foil in the NW synthesis experiments.

(reaction 6) for hours.

$$\text{Thermal annealing}: H_2Ti_8O_{17}NW \rightarrow 8TiO_2NW + H_2O \quad \text{(several hours)} \tag{6}$$

$$\text{Plasma exposure}: H_2Ti_8O_{17}NW + O \rightarrow 8TiO_2NW + H_2O + 0.5O_2 \ (5\ \text{min}) \tag{7}$$

In both cases bonds need to be broken and water molecules are removed by topotactic transformation[11] preserving the NW morphology. In thermal annealing, the bonds need to be broken and diffuse to surface of NW, recombine to form water vapor, and desorb from NW surface. In plasma exposure, the O radicals can diffuse and actively help break the bonds and also help with recombination reactions on the surface to release water and oxygen molecules from the NW surface. The oxygen radical mediation can enhance the kinetics of all elementary steps involved in the water molecule desorption for transforming titanate to TiO_2 NWs. Also plasma exposure (reaction 7) is more favorable than thermal annealing (reaction 6) by 174 kJ/mol based on based on ΔG calculations at 1200 K.

EDX analysis after ion exchange and annealing showed complete removal of K and Ti/O ratio matched with TiO_2. XRD spectrum of annealed NWs shows their phase to be rutile with lattice parameters of $a = b = 4.593$ Å and $c = 2.959$ Å and matches with JCPDS file number 65-0191 as shown in Figure S5a in Supporting Information. A sharp peak at 27.6° shows the characteristic of a highly crystalline rutile phase which is confirmed by HRTEM analysis. The rutile structure was also confirmed by Raman spectroscopy, which shows peaks at 447 and 611 cm^{-1} (Figure S5b in Supporting Information). Figure 5b shows the HRTEM image and corresponding SAED along the [001] zone axis of a TiO_2 NW. The TiO_2 NWs are single crystalline without any amorphous oxide layer, and from SAED their growth direction is determined to be [110] as shown in Figure 5b. The interplanar spacing of 3.2 Å in (110) planes (which are the most thermodynamically stable planes in the rutile), obtained from lattice fringes in Figure 5b, is in excellent agreement with *d*-spacing of (110) rutile planes. Also lattice fringe spacing of 4.6 Å along either (100) or (010) plane matches the lattice parameter (*a* or *b*) of the rutile TiO_2. In the case of thermal annealing, it has been shown to obtain different phases of TiO_2 by annealing at different temperatures. In this regard, detailed studies using plasma annealing are being conducted and will be reported later.

Mechanistic Studies to Understand Nucleation and Growth. Prior studies suggested that the 1D titanate structures formed due to a layered structure for titanates allowed "oriented attachment".[12,27−29] In one study, it was hypothesized to result from K_2O-rich liquid melt (of TiO_2 and alkali compound), but the 1D growth resulted from the melt quenching in 1D channels.[30] Another hypothesis predicted that the NWs grew by oriented relation between the crystallographic planes of anatase matrix and the titanate nuclei.[31] However, it is not clear the reasons for nucleation and 1D growth for layered titanate compared to two-dimensional and spherical shapes. Also, the factors that determine the resulting diameters are not understood. So, several experiments were conducted to understand the underlying role of alkali metals in the nucleation and growth of TiO_2 NWs during plasma oxidation. The analysis presented here can apply to many other circumstances in which alkali metal compounds are employed for synthesis of TiO_2 NWs such as the hydrothermal synthesis techniques.

Ti foil experiments using KCl (both crystal and solution forms) resulted in NWs but those using HCl did not. This experiment showed that Cl is not important for NW formation similar to that presented in the reference for thermal oxidation.[21] No NWs were obtained on Ti foil with only Ti powder on it without any KCl added. Further, NWs were obtained with KOH crystals illustrating that K indeed is responsible for NW growth. NWs were also obtained when using NaCl, NaOH, and LiCl crystals, thereby further confirming the generic role of alkali metals (Li, Na, K, etc.) for NW growth. Results from the experiments using different reagents are summarized in Figure 6. The experiment using a Ti foil with only half of the foil covered by KCl resulted in NWs on the part covered with KCl suggesting that the vapor form of K (or its transport) is not responsible for the NW growth.

In addition to the high density of nucleation and growth from large size, spherical Ti metal particles, the results with oxidation of Ti foils also indicate high density of NWs from hemispherical islands. As the islands become closely spaced, the resulting NWs grow vertically due to spatial confinement leading to vertical arrays as shown in Figure 7a. These observations are similar to those observed when performing plasma oxidation of low-melting point

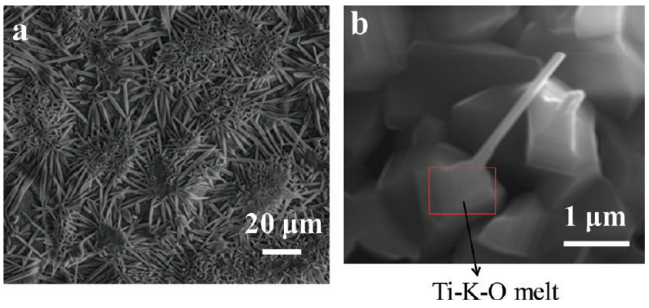

Figure 7. SEM images showing (a) NWs growing out from a molten metal pool on Ti foil, and (b) a NW emanating from molten melt below.

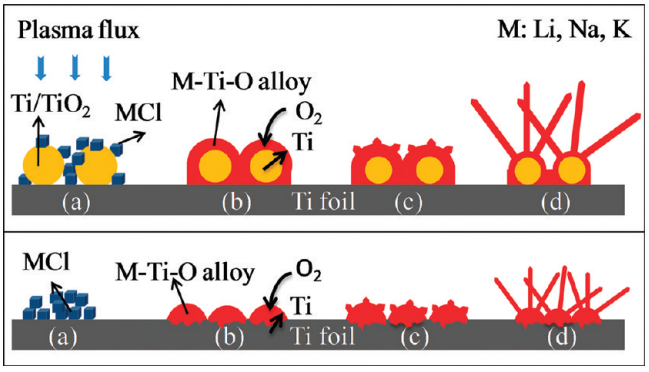

Figure 8. Schematic depicting the proposed growth mechanism for alkali metal-assisted (compounds involving Li, Na, or K) growth of TiO_2 NWs. The top scheme shows the NW formation when Ti or TiO_2 powder is used, while the bottom scheme depicts formation on Ti foil only. The steps are (a) feed mixture placed onto Ti foil, (b) alkali compound alloys Ti species to form K-Ti-O alloy, (c) supersaturation leading to titanate nuclei formation, and (d) basal growth of titanate NWs.

metal particles supported on substrates[13] which suggest that the nucleation and 1D growth occurs with nucleation out of a molten phase. On the basis of all the experimental observations (results in Figures 6 and 7) and our prior work with NW nucleation and growth from molten phases,[13,14,32] we postulate that the titanate NW formation follows four basic steps as shown in Figure 8: (1) formation and availability of alkali metal from its salt, (2) alloying of molten metal with Ti or TiO_2 to form Ti-alkali metal-O alloy which lowers the melting point of Ti due to eutectic formation, (3) continuous dissolution of Ti from below leading to phase segregation and bulk nucleation, and (4) basal growth of nuclei into NWs from dissolved species leading to 1D growth. In terms of specific experiments using KCl, under plasma exposure, KCl melts (at 775 °C) and spreads on the surface as a thin gray film. K vapor or melt can easily be oxidized to form K_2O which either decomposes at the synthesis temperatures (~450 °C is the decomposition temperature) or quickly alloys with Ti species. The availability of active K may be necessary for the growth of NWs. The molten K quickly alloys with Ti and O and starts dissolving underlying Ti by lowering its melting point due to eutectic formation. Further alloying of Ti in K-Ti-O melt leads to supersaturation and bulk nucleation of potassium titanate nuclei out of the molten phase. Data on the K-Ti-O phase diagram are scarce; however, from one report[30] the $K_2Ti_8O_{17}$ phase is predicted to nucleate at temperatures greater than 1200 °C and Ti/K ratio in excess of 20. The predicted temperature may not be accurate as

Table 1. Comparison of Parameters Affecting the TiO_2 NW Formation in Different Alkali Metal Assisted Plasma Exposure Experiments

NW formation time	KCl: 5 min	NaCl: 13 min	LiCl: 8 min
oxide decomposition temperature	K_2O: 450 °C	Na_2O: ~1000 °C	Li_2O: ~1350 °C
melting point (°C)	K: 63	Na: 98	Li: 180
ionic radii (pm): $Z = 6$	K^+: 138	Na^+: 102	Li^+: 74

lower synthesis temperatures have been reported.[24] In our case, the NW synthesis temperature at the surface of the foil can be as high as 1000 °C due to plasma gas temperatures. An approximate calculation on the critical nucleus size of the titanate phase using classical nucleation theory for solute precipitation from dissolved solution[14] predicts it to be in the tens of nanometer range which matches with the experimental observations. A K-Ti phase diagram available in the literature shows very low solubility (<0.0003 at%) for Ti in K.[33] Even for a K-Ti-O system, the same can be applied to conclude that the solubility would be very less between the K-rich melt and the Ti-rich titanate phase. The contact angle between solid titanate phase nuclei and K-rich melt is approximately calculated to be 120° (nonwetting contact angle) based on the Neumann approach,[34] and using average surface energy values of 83.4 mJ/m^2 and 174 mJ/m^2 for titanate[35] and K-rich melt[36] respectively, which confirms the poor wettability. Thus, poor miscibility and wettability ensure that the further dissolution of Ti in the Ti-K-O melt leads to 1D NW growth perpendicular to the molten surface and not the lateral crust formation. Also, the growth occurs predominantly from the underlying Ti foil/powder (as shown in Figure 7b) and not from TiO_2 in the vapor phase because the growing NWs are still attached to their molten base. Another thing to note is that the titanate nucleation and subsequent NW growth is not uniform throughout the foil but occurs locally at the areas (on the foil) selectively wetted by the melt. Also, in the case of large Ti metal particle size (65 μm) alkali metal dissolution and alloy formation only occurs to a depth of a few micrometers from the Ti surface with underlying sphere core intact. But, in the case of smaller size (32 nm) TiO_2 powders complete consumption of sphere is observed. The growth mechanism is schematically represented for oxidation of foils and powders in Figure 8.

The ease of NW formation using chlorides of alkali metals (Li, Na, and K) was compared in light of their respective melting points of alkali metals, oxide decomposition temperatures, and ionic radii. Table 1 lists these parameters and shows that NW formation time follows the pattern: K < Li < Na. It appears that the KCl-assisted NW formation is easiest and fastest because of a low melting point of K compared to Li and Na and also its respective oxide decomposes very easily. Between Li and Na based NW formation time, the former seems to be a bit easier because of its smaller and comparable ionic radii (Ti^{4+} = 61 pm, when Z = 6), though both of them have similar oxide decomposition temperatures. It should also be noted that chlorides of all these alkali metals have melting points in the range of 605–801 °C, which is well below the synthesis temperature (~1000–1500 °C).

Group II elements were also tested as reagents for TiO_2 NW formation on Ti foil. However, no NWs were seen when $CaCl_2$ was used instead of KCl under similar conditions. In this case laterally grown crystals were seen on the Ti metal surface (Figure 6f).

This behavior can be explained by the reasons opposite to the KCl case. $CaCl_2$ melts (at 772 °C) to form CaO in atmospheric plasma. CaO does not decompose at the synthesis temperatures (~1500 °C) and along with Ti results in the formation of three-phase region with different Ti−Ca−O compounds.[37] Ca unlike K is not low melting point metal either (839 vs 63 °C). Although the growth mechanism in hydrothermal method is not clear, we hypothesize that it follows the exact same mechanism as proposed above and hence our method can be applicable to other NW systems that have been synthesized using hydrothermal methods to date.

CONCLUSIONS

Titanate NWs resulted using atmospheric plasma exposure of either Ti or TiO_2 powders or foils in the presence of various alkali metal salts. The synthesis time scale is very fast, and this method is suitable for large-scale production of NWs. The 1D growth occurs with bulk nucleation and basal growth of nuclei from molten alloys of alkali metal-Ti-O similar to that of direct oxidation of low-melting metals for respective metal oxide NWs. In the experiments specifically using KCl, as-synthesized potassium titanate ($K_2Ti_8O_{17}$) NWs were obtained. A simple procedure of ion exchange with HCl followed by annealing converted potassium titanate NWs to rutile phase TiO_2 NWs. Plasma annealing is shown to reduce the time scales to minutes compared to hours required for the thermal annealing step.

ASSOCIATED CONTENT

Supporting Information. A graph showing the theoretical equilibrium gas phase composition of Ti-containing species; SEM images of preliminary results with TiO_2 without any KCl and results with TiO_2 powder on both Ti foil and in direct gas phase setup; elemental composition of as-synthesized titanate NWs; XRD and Raman spectra of rutile phase TiO_2 NWs. This material is available free of charge via the Internet at http://pubs.acs.org.

AUTHOR INFORMATION

Corresponding Author

*E-mail: mahendra@louisville.edu. Tel.: 502-852-8574. Fax: 502-852-6355.

ACKNOWLEDGMENT

Authors gratefully acknowledge support from Department of Energy (DE-FG02-07ER46375) and KY Renewable Energy Consortium (KREC) through DOE Grant No. DE-FG36-05GO85013 and also acknowledge support from Kentucky Commercialization Fund (KSTC-144-401-10-044) on the reactor development effort and a Phase I grant from NSF SBIR program (IIP-1047215). One of the authors (M.K.S) founded the company (Advanced Energy Materials, LLC) to commercialize the technology.

REFERENCES

(1) Adachi, M.; Murata, Y.; Takao, J.; Jiu, J.; Sakamoto, M.; Wang, F. *J. Am. Chem. Soc.* **2004**, *126*, 14943.
(2) Armstrong, G.; Armstrong, A. R.; Bruce, P. G.; Reale, P.; Scrosati, B. *Adv. Mater.* **2006**, *18*, 2597.
(3) Francioso, L.; Taurino, A. M.; Forleo, A.; Siciliano, P. *Sens. Actuators B: Chem.* **2008**, *130*, 70.
(4) Khan, S. U. M.; Sultana, T. *Solar Energy Mater. Solar Cells* **2003**, *76*, 211.
(5) Gubbala, S.; Chakrapani, V.; Kumar, V.; Mahendra, K.; Sunkara *Adv. Funct. Mater.* **2008**, *18*, 2411.
(6) Hoyer, P. *Langmuir* **1996**, *12*, 1411.
(7) Lakshmi, B. B.; Patrissi, C. J.; Martin, C. R. *Chem. Mater.* **1997**, *9*, 2544.
(8) Kasuga, T.; Hiramatsu, M.; Hoson, A.; Sekino, T.; Niihara, K. *Langmuir* **1998**, *14*, 3160.
(9) Li, G. L.; Wang, G. H. *J. Mater. Res.* **1999**, *14*, 3346.
(10) Zhang, Y. X.; Li, G. H.; Jin, Y. X.; Zhang, Y.; Zhang, J.; Zhang, L. D. *Chem. Phys. Lett.* **2002**, *365*, 300.
(11) Liu, B.; Boercker, J. E.; Aydil, E. S. *Nanotechnology* **2008**, *19*, 505604.
(12) Peng, X.; Chen, A. *Adv. Funct. Mater.* **2006**, *16*, 1355.
(13) Sharma, S.; Sunkara, M. K. *J. Am. Chem. Soc.* **2002**, *124*, 12288.
(14) Sunkara, M. K.; Sharma, S.; Miranda, R.; Lian, G.; Dickey, E. C. *Appl. Phys. Lett.* **2001**, *79*, 1546.
(15) Mozetic, M.; Cvelbar, U.; Sunkara, M. K.; Vaddiraju, S. *Adv. Mater.* **2005**, *17*, 2138.
(16) Cvelbar, U.; Chen, Z.; Sunkara, M. K.; Mozetič, M. *Small* **2008**, *4*, 1610.
(17) Wu, J.-M.; Shih, H. C.; Wu, W.-T. *J. Vac. Sci. Technol. B* **2005**, *23*, 2122.
(18) Lau, M.; Dai, L.; Bosnick, K.; Evoy, S. *Nanotechnology* **2009**, *20*, 025602.
(19) Park, J.; Ryu, Y.; Kim, H.; Yu, C *Nanotechnology* **2009**, *20*, 105608.
(20) Hong, Y. C.; Kim, J. H.; Bang, C. U.; Uhm, H. S. *Phys. Plasmas* **2005**, *12*, 114501.
(21) Cheung, K. Y.; Yip, C. T.; Djuriscaroni, A. B.; cacute; Leung, Y. H.; Chan, W. K. *Adv. Funct. Mater.* **2007**, *17*, 555.
(22) Kumar, V.; Kim, J. H.; Pendyala, C.; Chernomordik, B.; Sunkara, M. K. *J. Phys. Chem. C* **2008**, *112*, 17750.
(23) Kim, J. H.; Kumar, V.; Chernomordik, B.; Sunkara, M. K. *Inf. Midem (J. Microelectron. Electron. Compon. Mater.)* **2008**, *38*, 237.
(24) Yuan, Z. Y.; Zhang, X. B.; Su, B. L. *Appl. Phys. A: Mater. Sci. Process.* **2004**, *78*, 1063.
(25) Wang, B. L.; Chen, Q.; Hu, J.; Li, H.; Hu, Y. F.; Peng, L. M. *Chem. Phys. Lett.* **2005**, *406*, 95.
(26) Sun, X.; Chen, X.; Li, Y. *Inorg. Chem.* **2002**, *41*, 4996.
(27) Tsai, C.-C.; Teng, H. *Chem. Mater.* **2005**, *18*, 367.
(28) Wang, B.; Shi, Y.; Xue, D. *J. Solid State Chem.* **2007**, *180*, 1028.
(29) Lee, C. T.; Um, M. H.; Kumazawa, H. *J. Am. Ceram. Soc.* **2000**, *83*, 1098.
(30) Bao, N.; Feng, X.; Lu, X.; Yang, Z. *J. Mater. Sc.* **2002**, *37*, 3035.
(31) Du, G. H.; Chen, Q.; Han, P. D.; Yu, Y.; Peng, L. M. *Phys. Rev. B* **2003**, *67*, 035323.
(32) Chandrasekaran, H.; Sumanasekara, G. U.; Sunkara, M. K. *J. Phys. Chem. B* **2006**, *110*, 18351.
(33) Bale, C. *J. Phase Equilib.* **1989**, *10*, 134.
(34) Drelich, J.; Miller, J. D. *J. Colloid Interface Sc.* **1994**, *167*, 217.
(35) Yuchun, O.; Feng, Y.; Jin, C. *J. Appl. Polym. Sc.* **1997**, *64*, 2317.
(36) Sato, Y.; Ejima, T.; Fukasawa, M.; Abe, K. *J. Phys. Chem.* **1990**, *94*, 1991.
(37) Jacob, K. T.; Gupta, S. *Bull. Mater. Sci.* **2009**, *32*, 611.